Local Damage Detection in Beam-Column Connections Using a Dense Sensor Network

Elizabeth L. Labuz[1], Minwoo Chang[2], and Shamim N. Pakzad[3]

[1]Graduate Student, Department of Civil and Environmental Engineering, Lehigh University, 117 ATLSS Drive, Bethlehem, PA 18015; PH (610) 758-4543; FAX (610) 758-5553; email: elabuz@lehigh.edu
[2]Graduate Student, Department of Civil and Environmental Engineering, Lehigh University, 117 ATLSS Drive, Bethlehem, PA 18015; PH (610) 758-6273; FAX (610) 758-5553; email: mic307@lehigh.edu
[3]P.C. Rossin Assistant Professor, Department of Civil and Environmental Engineering, Lehigh University, 117 ATLSS Drive, Bethlehem, PA 18015; PH (610) 758-6978; FAX (610) 758-5553; email: pakzad@lehigh.edu

ABSTRACT

Damage prognosis for structural health monitoring is a challenging and complex research topic in civil engineering. Critical components of damage detection are identifying the location and severity of damage in a structure, as well as its global effect on the structure. Local damage can increase over time and have additional adverse effects on the entire structure. Traditional damage detection methods using sensor data are effective in recognizing the change in global properties of a structure. However, these methods are neither effective nor sensitive in identifying local damage. The use of dense clustered sensor networks provides promising applications in analysis of structural components and identifying local damage. In this study, a prototype beam-column connection was constructed and instrumented by a dense sensor network. The column ends of the test specimen have fixed connections, and the beam cantilevers from the centerline of the column. The beam was excited with an actuator at its free end, and accelerometer sensors measured the response of the members to dynamic excitations at several locations along the specimen. The response at each sensor location was compared to that of other locations and pair-wise influence coefficients were estimated. Damage is introduced to the system by replacing a portion of the beam element with a smaller section, and thus reducing its stiffness. New influence coefficients were calculated and compared to the undamaged values. By statistically comparing the change in influence coefficients, the damage is accurately and effectively identified.

INTRODUCTION

Structural health monitoring (SHM) plays an integral role in maintaining the integrity of important civil, mechanical, and aerospace engineering systems. Structures experience a number of dynamic influences on a daily basis ranging from typical ambient vibrations to more extreme wind and earthquake loadings. Whether the damaging effects of these load cases are visible immediately or appear more gradually in time, it is important to be able to detect the damage before it becomes too

detrimental to the entire structure and its surroundings. Not only will money be saved in being able to repair more manageable damages at earlier detection, but also fatal catastrophes can be prevented. As a number of structures are beginning to reach the limit of their service lives, the need for effective, efficient, and affordable damage detection methods is becoming more and more apparent.

Traditional non-destructive evaluation (NDE) techniques include but are not limited to visual inspection, liquid penetrant, magnetic particle, radiography, eddy currents, ultrasonic waves, acoustic emission, and infrared thermography (Trimm 2007). While these methods can be useful in certain circumstances, they require *a priori* knowledge of the location of damage and are also subject to the trained eye of the inspector. Also, in order to implement these techniques one must have direct access to the location of damage, which may be difficult to reach. Furthermore, NDE techniques are be costly, difficult to use with complex equipment, and provide only a temporary means of SHM.

Both advancements in sensor technologies as well as improved understanding of the modal properties of structures have given rise to vibration-based damage identification methods. These methods find a basis in the vibration behavior of a structure, namely the connection between the modal parameters of a structural system—natural frequencies, mode shapes, and modal damping—and its physical properties—mass, stiffness, and damping (Doebling *et al* 1998; Alvandi and Cremona 2006). Parametric changes signify changes in the physical properties, i.e. structural damage in the form of mass or stiffness loss. Also, the advancements of wireless networks make it possible to implement these vibration-based methods on a semi-permanent basis for continual monitoring of structures.

However, current SHM practices involving global-based damage detection require knowledge of specific structural properties, including mass, stiffness, or damping ratio, for which it is often difficult to determine correct values (Koh *et al* 1995; Morassi and Rovere 1997; Sohn and Law 1997; and Ratcliffe 1997). Additionally, global detection techniques, which are based on global properties, are not sensitive to local damage and, therefore, cannot identify damage or determine its locations. Other proposed local damage detection methods, for example the damage locating vector (DLV) method (Bernal 2002), also require the knowledge of structural properties, or require homogeneity of the structural properties as in the two-dimensional gapped smoothing method (Yoon *et al* 2005).

This paper presents an effective damage detection method that uses vibration responses collected via densely clustered sensors to achieve localized damage detection without the need for exact knowledge of structural properties. Influence coefficients, obtained from linear regression between every two node responses, are used as the index for determining the existence of damage. The accuracy of these coefficients is confirmed by considering both estimation accuracy and normalized estimation error. The change point of time-variant influence coefficients can also be determined using a Bayesian statistical framework.

The effectiveness of influence coefficient as a damage indicator is demonstrated through simulated examples as well as laboratory experiments. An OpenSees model was implemented to demonstrate the use of this algorithm as applied to a simple beam-column connection, simulating a local joint, subjected to damage.

Laboratory experiments were performed on a prototype of a similar beam-column connection with unknown structural properties subjected to different loading profiles. Both the simulated and experimental results, combined with the investigation of estimation accuracy and normalized estimation error, support the efficacy and reliability of this proposed method in detecting damage and its location on a local scale.

METHODOLOGY

Influence Coefficients and Normalized Estimation Error. The algorithm employed in this paper, which is outlined in Figure 1, utilizes regression analysis to determine the pair-wise relationship between node responses in order to predict the location of structural damage. By calculating influence coefficients, α_{ij}, between two nodes *i* and *j*, based on vibration-induced acceleration response data, one can determine the correlation between these responses as follows:

$$u_j(t_k) = \alpha_{ij} \cdot u_i(t_k) + \varepsilon_{ij}(t_k).$$

The comparison of the resulting influence coefficients from the initial undamaged state with that of the damaged state of the structure serves as a "damage indicator" when it yields a significant change in the value of the coefficients from state to state. More specifically, the influence coefficients exhibit a much more significant change when nodes *i* and *j* are located on opposing sides of the damaged segment versus when they are on the same side. This characteristic allows for the identification of the damage location by comparing which influence coefficients exhibit significant changes.

Once the coefficients have been calculated the accuracy of the data must be assessed and verified before damage detection can be performed. This is done through consideration of both the accuracy of the pair-wise coefficients and the estimation error. The product of influence coefficients α_{ij} and α_{ji}, yields the evaluation accuracy, EA_{ij}, of these coefficients, indicating which node responses are linearly related to one another with the least amount of error, ε_{ij}, and thus are more accurate predictors. An evaluation accuracy of 1.0 signifies a strong accuracy of estimation, while a product of less than 1.0 corresponds to progressively higher values of noise and nonlinear behavior of the physical structure.

The second parameter that is used for data verification is normalized estimation error, which is calculated by

$$\gamma_{ij} = \frac{\sigma_{\alpha_{ij}}}{\alpha_{ij}}.$$

Normalized estimation error allows for a direct comparison of the amount of error associated with the estimation of each influence coefficient as a damage indicator. This parameter is used to determine which influence coefficients should be used for damage detection. A low estimation error will correspond to a more accurate predictor. Once the accuracy and error have been assessed for each coefficient, post-processing of the data can be performed for damage identification and localization.

Statistical Framework. The final portion of this damage detection algorithm applies a statistical framework. A Bayesian statistic is used to determine the change point (Chen and Gupta 2000), the point at which the data indicates damage, at 95% confidence level. This statistical inference method tests the hypothesis,

$$H_0: \alpha_1 = \alpha_2 = \cdots = \alpha_N = \bar{\alpha},$$

against the one-sided alternative hypothesis,

$$H_A: \alpha = \alpha_1 = \alpha_2 = \cdots = \alpha_r < \alpha_{r+1} = \cdots = \alpha_N.$$

The variables r, representing the change point at which the parameter α may have changed, mean μ, and standard deviation σ are all unknown. N represents the number of tests. The Bayesian statistic that is used is

$$S_N = \sum_{i=1}^{N-1} i(\alpha_{i+1} - \bar{\alpha}).$$

Because the standard deviation is unknown, it is estimated as the standard error, $\hat{\sigma}$. The statistic that is used to test the aforementioned hypothesis is

$$t = \frac{S_N}{\hat{\sigma}\sqrt{\frac{N(N-1)(2N-1)}{6}}}$$

and has a t-distribution with N-2 degrees of freedom. The confidence level to which this hypothesis is tested can be designated as desired. The examples presented in this paper assume the commonly used 95% confidence level. The physical significance of this hypothesis test is such that the alternative hypothesis, H_A, indicates that the structure has incurred damage, while the null hypothesis, H_0, means that there is not adequate evidence to establish that damage exists. These hypotheses are tested for those node pairs that have been identified as significant damage indicators in the assessment and verification stage of the method.

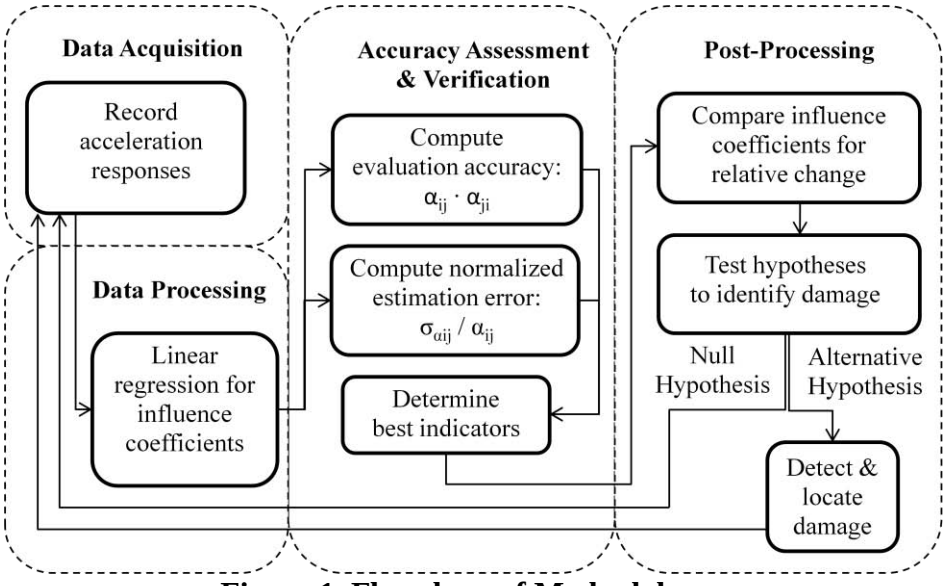

Figure 1. Flowchart of Methodology.

SIMULATED EXAMPLE

The algorithm was first validated using a simulated model of a beam-column connection, representing a local joint. The simulation was created using OpenSees software (Mazzonih *et al.* 2000). The model has two members (representing the portion of the beam and column close to the connection) of uniform, hollow, square cross-section with 3.05 mm thickness, 272.5 mm^2 area, and a moment of inertia of 23,114 mm^4. The steel is assumed to have an elastic modulus of 200 GPa. The structure is assumed to be massless, as one assumption of the method is that the mass has negligible effect on the performance of the algorithm. The boundary conditions of the column are fixed on either end, while the beam cantilevers from the centerline of the column. Two simulations were performed including an undamaged condition, the properties of which have been described, and a damaged condition. Damage was simulated by reducing the beam stiffness by 40%. The damaged properties of the beam include a wall thickness of 1.52 mm, a cross-sectional area of 145.5 mm^2 to a moment of inertia of 13,885 mm^4. For each of these models, displacement data was simulated for a white noise excitation applied at the free end of the beam, and responses were collected for each of the nine node locations designated along the beam and column as shown in Figure 2. Measurement noise was also accounted for by adding a Gaussian noise with a standard deviation equal to 5% of the root mean square of each response signal.

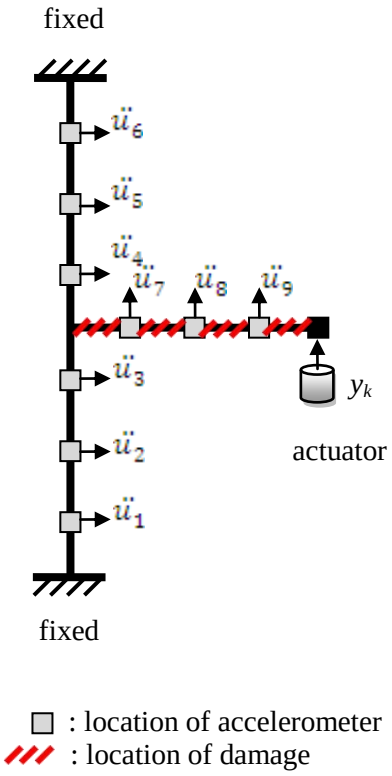

Figure 2. Simulated model of beam-column connection with nine node locations.

The algorithm was then applied to simulated data and the parameters were extracted. The relative change in the influence coefficients between the undamaged and damaged states is shown for each pair-wise node relationship in Table 1. The influence coefficients $\alpha_{ij},\ 1 \leq i,j \leq 6$ all experience very small (less than 1%) changes between the undamaged and damaged states. This implies that the physical properties between these nodes have not changed. However, the coefficients of nodes 1 through 6 paired with nodes 7, 8, and 9 show relative changes of between 30-40%. When nodes are on opposite sides of the damage, i.e. nodes 1 through 6 are located on the undamaged column, while nodes 7, 8 and 9 are located on the damaged beam, the physical properties between the paired nodes changes. This physical change is reflected in a more significant relative change in the value of influence coefficients. Furthermore, the influence coefficients $\alpha_{ij},\ 7 \leq i,j \leq 9$ also experience a noticeable change in coefficients (about 3-10%). This signifies that the physical properties of the structure between α_{78}, α_{79}, and α_{89} have changed. Therefore, damage must exist between these nodes. This is consistent with the simulated damage: a 40% stiffness reduction of the beam.

Table 1. Relative change in influence coefficients, α_{ij}, for simulated structure.

	1	2	3	4	5	6	7	8	9
1		0.24%	0.12%	0.03%	0.12%	0.09%	30.6%	39.5%	43.3%
2	-0.23%		-0.10%	-0.19%	-0.12%	-0.14%	30.3%	39.2%	43.0%
3	-0.12%	0.13%		-0.06%	-0.01%	-0.04%	30.5%	39.4%	43.1%
4	-0.06%	0.19%	0.08%		0.07%	0.03%	30.6%	39.5%	43.2%
5	-0.11%	0.12%	-0.01%	-0.07%		-0.03%	30.5%	39.4%	43.1%
6	-0.07%	0.16%	0.04%	-0.04%	0.03%		30.5%	39.4%	43.2%
7	-23.4%	-23.3%	-23.4%	-23.4%	-23.4%	-23.4%		6.81%	9.70%
8	-28.3%	-28.2%	-28.3%	-28.3%	-28.2%	-28.3%	-6.38%		2.71%
9	-30.2%	-30.1%	-30.1%	-30.2%	-30.1%	-30.2%	-8.85%	-2.63%	

EXPERIMENTAL SETUP

The algorithm was further verified through laboratory experiments on a specimen similar to that of the simulated model. The connection was constructed such that the two ends of the column have fixed supports, while the beam cantilevers from the centerline of the column. Again, the prototype represents a portion of the beam and column members as they come to a local joint. There were nine accelerometer sensor locations on the specimen, as shown in Figure 3. The free end of the cantilever was attached to an actuator and excited by harmonic force at various dictated frequencies—5 Hz, 10 Hz, 15 Hz, and 20 Hz—and the acceleration responses were collected at each of the nine sensor nodes. The influence coefficients were then computed. This portion of the experiment served to establish a base response for the undamaged structure.

For the second portion of the experiment, the beam member was replaced by a member of 40% reduced wall thickness in order to simulate damage to the structure. The excitations were repeated, and the damaged state influence coefficients were

computed. The resulting data was then compared between the damaged and undamaged states to verify the detection of damage.

Data was collected at a 200 Hz sampling rate and 0.005 sec time step, with each test lasting 10 seconds total. Both the undamaged and damaged structures were tested 50 times, for a total of 100 tests, each containing 2000 data points per sensor location. These 1.8 million data points were then processed through the algorithm to detect the occurrence of damage.

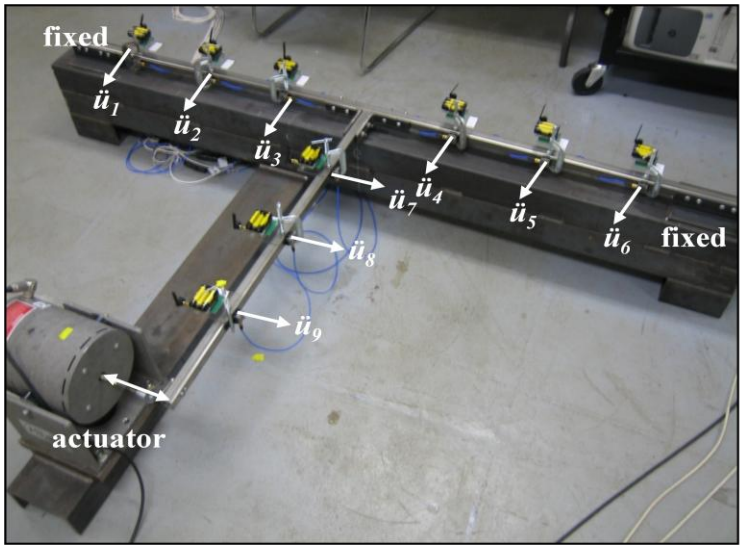

Figure 3. Experimental beam-column prototype.

DISCUSSION OF RESULTS

The experiments were conducted with the undamaged and damaged states at four different forcing frequencies: 5 Hz, 10 Hz, 15 Hz, and 20 Hz harmonic vibrations. While the algorithm is applicable for data resulting from all four frequencies, the 15 Hz data exhibited the least amount of actuator noise error, and thus is presented hereafter.

Accuracy Assessment and Verification. Once the 72 influence coefficients have been calculated from the acceleration data, the data must be assessed to identify the most significant indicators, which will be used for damage detection. This involves two parameters: evaluation accuracy, *EA*, and normalized estimation error, γ. By inspection of these parameters, eight different trends can be identified in the undamaged and damaged parameters, with lower estimation errors coinciding with greater evaluation accuracies and vice versa. These trends have been designated as eight different regions, whose mean values are presented in Table 2. Region 1 in the table corresponds to the least estimation error and highest accuracy, and region 8 corresponds to the greatest estimation error and lowest accuracy. Parameters in region 1, consisting of $\alpha_{ij},\ 7 \leq i,j \leq 9$, are the most accurate and have the least error. This is a reasonable outcome as nodes 7, 8, and 9 are all located in a row along the same

structural element (the beam). Therefore, the accelerations at node 7, for example, will be more highly correlated to those at node 8 or 9.

On the contrary, region 8, which consists of parameter α_{16}, exhibits the poorest accuracy and the greatest estimation error. This can be accounted for by the fact that each of these nodes is located at either end of the column near the fixed connections. These boundary conditions create large additional noise, which contributes to the fact that α_{12} or α_{56} exhibit lower accuracy than α_{78} or α_{89} despite the similar configuration of the nodes with respect to one another. Figures 4(i) and (ii) show an example of α, *EA*, and γ results from regions 1 and 8, respectively. Figure 4(i) shows that the *EA* is almost equal to unity and the γ is almost equal to 0 for region 1, while Figure 4(ii) shows a much lower *EA* and a noticeably higher γ for region 8. Based on similar data for all 8 regions, it can be concluded that regions 1 through 3 contain useful damage indicators. On average, these influence coefficients exhibit accuracy greater than 95% and estimation error less than .0044.

Table 2. Average Estimation Error (γ) and Evaluation Accuracy (*EA*).

Region	Influence Coefficients	γ_{ij} Average	EA_{ij} Average
1	α_{78}, α_{79}, and α_{89}	0.0002	0.9999
2	α_{23} and α_{45}	0.0015	0.9947
3	α_{27}, α_{28}, α_{29}, α_{37}, α_{38}, α_{39}, α_{47}, α_{48}, α_{49}, α_{57}, α_{58}, and α_{59}	0.0044	0.9554
4	α_{12}, α_{13}, α_{46}, and α_{56}	0.0057	0.9377
5	α_{17}, α_{18}, α_{19}, α_{67}, α_{68}, and α_{69}	0.0074	0.8997
6	α_{24}, α_{25}, α_{34}, and α_{35}	0.0093	0.8379
7	α_{14}, α_{15}, α_{26}, and α_{36}	0.0114	0.7903
8	α_{16}	0.0161	0.6626

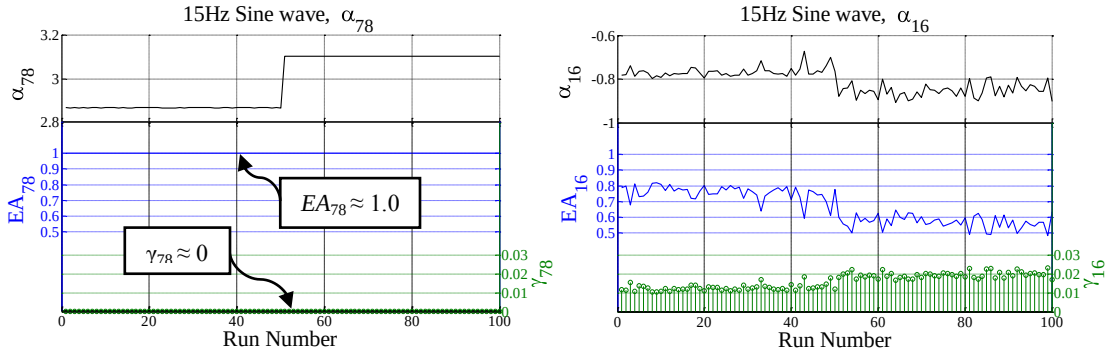

(i) **(ii)**

Figure 4. Comparison of α, *EA*, and γ Results: (i) Region 1 and (ii) Region 8.

Post-Processing and Damage Detection. The results of the relative changes in the influence coefficients, α_{ij}, from the 15 Hz harmonic excitation of the undamaged and damaged tests are shown in Table 3. Observing these coefficient changes is the first step in post-processing the data. The changes associated with α_{78}, α_{79}, and α_{89}, which are 8%, 12%, and 4% respectively, are indicators of a property change between nodes

7 and 9. This is consistent with the damage, or stiffness reduction, that was created along the full length of the beam portion of the test structure.

The coefficients of region 2, α_{23} and α_{45}, experienced 3% and 8% changes. This is less consistent with what would be expected in comparison to the very low (less than 1%) changes that were seen in the simulated results. One major cause of this is noise, which is difficult to control in an experimental setting, but even more so in a real structure.

Influence coefficients from region 3 were more in line with the prediction of the simulated results, with the exception of α_{49} (2%) and α_{57} (3%), which were low compared to the 5-40% range of the others. Again, these two discrepancies are likely accountable to noise. However, the majority of the coefficients in this region showed noticeable fluctuations from the undamaged state to the damaged state. These changes, along with the model results, show that nodes on opposite sides of the damage location experience the largest changes. This is because as damage occurs, the relationship of two points in the actual physical structure deviates slightly from linear behavior. Again, the changes in coefficients point to the location of damage in the structure (i.e. damage between nodes 2 and 7, 3 and 8, and so forth).

While the results for the first three regions were mostly consistent with the expectations set out by the simulated structure, the remaining regions were not as consistent. A prime example is region 6, consisting of parameters α_{24}, α_{25}, α_{34}, and α_{35}. According to the model, these coefficients, whose nodes are all located on the same side of the damage, should experience very little fluctuation from the undamaged to damaged states. However, their experimental changes range from 12-20%. Recall that in the previous verification stage region 6 showed the third lowest accuracy and the third highest error.

Table 3. Relative change in influence coefficients, α_{ij}, for experimental structure.

	1	2	3	4	5	6	7	8	9
1		2.3%	5.6%	17.9%	12.1%	11.2%	19.7%	29.5%	34.6%
2	0.5%		2.9%	19.8%	14.6%	16.4%	22.4%	32.5%	37.7%
3	1.3%	2.2%		16.4%	12.4%	14.5%	22.7%	32.9%	38.1%
4	36.8%	36.9%	41.8%		8.4%	7.0%	12.7%	5.5%	1.8%
5	28.7%	28.5%	33.4%	8.6%		1.8%	3.0%	5.0%	9.0%
6	32.3%	30.4%	35.0%	5.6%	2.5%		5.4%	2.4%	6.4%
7	22.7%	22.3%	26.0%	5.2%	1.5%	0.4%		8.3%	12.5%
8	28.6%	28.3%	31.7%	2.8%	9.0%	7.3%	7.6%		3.9%
9	31.2%	30.9%	34.2%	6.5%	12.4%	10.8%	11.1%	3.8%	

A further comparison of the simulated and experimental results for select coefficients is show in Figure 6. From this schematic it is evident that the results of the experiments were not as symmetric as the simulation suggested. Specifically, α_{25} and α_{58} were inconsistent between the simulated and experimental cases. For example, the experimental α_{25}, which belongs to region 6, suggests that damage exists between the nodes 2 and 5, which is not the case. Thus, this example, in conjunction with the results in Table 3, shows the importance of using parameters *EA* and γ to identify accurate damage indicators.

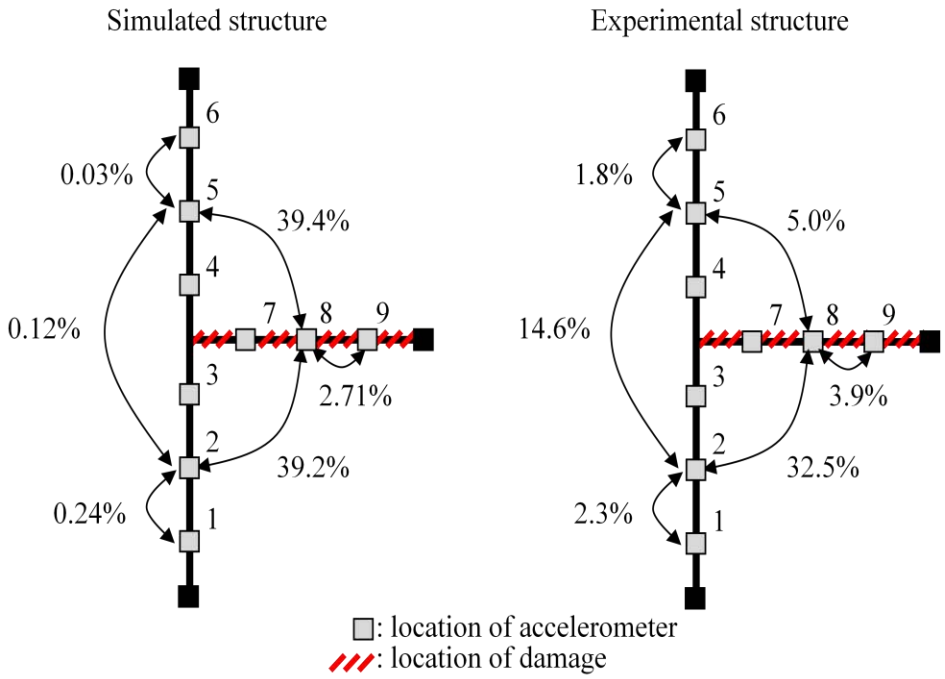

Figure 3. Comparison of relative change of coefficients between simulated and experimental structures.

As is evident, the difference between undamaged and damaged structures can be indicative of the existence and location of the damage. However, in an actual structure, one will not necessarily know when damage has occurred, or if in fact damage has occurred at all. Therefore, another element must be added for complete damage detection: the statistical framework.

The hypothesis testing graphically shows the change point of damage, the point at which damage is identified at a certain confidence level, by plotting the test statistic against the test run number. A graph in which the data crosses the confidence bounds, either positive or negative, corresponds to a positive hypothesis, previously defined as H_A, indicating the detection of damage. If the accuracy and estimation error associated with the nodes being considered are high and low respectively, the prediction of the hypothesis test will be more exact and will cross the confidence bounds closer to the occurrence of damage. In order to demonstrate this behavior, the test statistic from the 50 damaged state tests were plotted against their run number. Because damage exists for all of the plotted data, the most accurate damage indicators will yield a plot in which the confidence bounds are crossed closest to the occurrence of damage. This can be seen in comparing Figures 6(i) and (ii), the hypothesis test results for a region 1 coefficient, an accurate indicator, versus that of a region 8 coefficient, a poor indicator. The plot in Figure 6(i) crosses the 95% confidence bound much sooner than that of Figure 6(ii). Furthermore, these plots also demonstrate that damage is detected by hypothesis testing, although less precisely, for even the poorest damage indicating coefficient. Therefore, this method is a reliable means of damage detection.

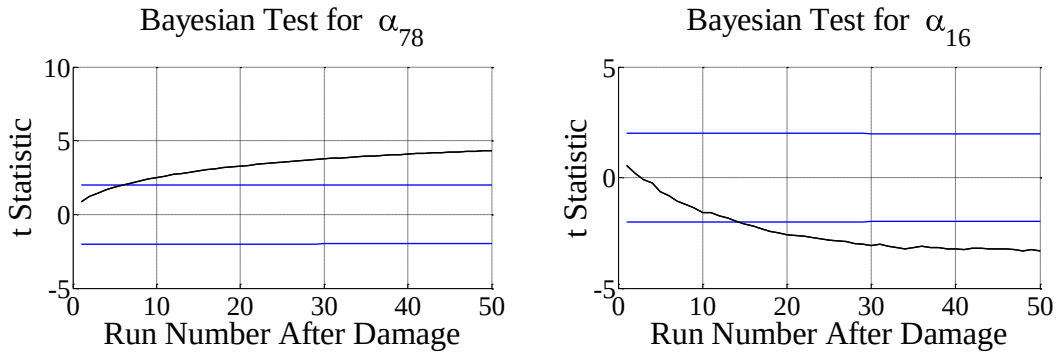

(i) **(ii)**

Figure 6. Comparison of Hypothesis Test Results: (i) Region 1 and (ii) Region 8.

CONCLUSION

In this paper, a densely clustered sensor network was successfully implemented for local damage detection of both a simulated model as well as an experimental prototype of a steel beam-column connection. Linear regression was used to estimate influence coefficients from vibration-induced acceleration responses of the structure. Two parameters, evaluation accuracy and normalized estimation error, demonstrated that certain influence coefficients are more reliable damage indicators than others. The influence parameters change when the structural properties change due to damage, such as a reduction in stiffness or mass. Therefore, this change point was used to detect and locate this damage. This method was verified through its application to a simulated model and an experimental prototype, both of which represented the local joint of a steel beam-column connection with nine sensor nodes. Damage equivalent to a 40% reduction in stiffness was created in a portion of the beam close to the joint for comparison to the initial state of the structures. The simulated model was excited by white noise, while the experimental model was excited by harmonic force at various forcing frequencies. The experimental acceleration data was then compared to the simulated response data. Although the experimental structure exhibited more noise error than the simulated results, both the simulation and the experiments identified the same influence coefficients (parameters in regions 1, 2, and 3) as the most reliable damage indicators. By statistically comparing these influence coefficients, damage was accurately and effectively diagnosed to a 95% confidence bound.

ACKNOWLEDGMENTS

The research described in this paper is supported by the National Science Foundation through Grant No. CMMI-0926898 by Sensors and Sensing Systems program. The authors thank Dr. Shih-Chi Liu for his support and encouragement.

REFERENCES

Alvandi, A., and Cremona, C. “Assessment of vibration-based damage.” *Journal of Sound and Vibration* 292 (2006) 179–202.

Bernal, D., M.ASCE. "Load Vectors for Damage Localization." *Journal of Engineering Mechanics* (Jan 2002): 7-14.

Chen, J., and Gupta, A.K. (2000). *Parametric change point analysis*. Birkhäuser, Boston.

Doebling, Scott W., Farrar, Charles R., and Prime, Michael B. "A Summary Review of Vibration-Based Damage Identification Methods." *The Shock and Vibration Digest* 30 (Mar 1998): 91-105.

Koh, C.G., See, L.M., and Balendra, T. "Damage Detection of Buildings: Numerical and Experimental Studies." *J. Struct. Engrg.* 121(8), (Aug 1995): 1155-1160.

Mazzonih, S., McKenna, F., Scott, M.H., and Fenves, G.L. (May 2009). *OpenSees Command Language Manual.* <http://opensees.berkeley.edu/OpenSees/manuals/usermanual/index.html>.

Morassi, A., and Rovere, N. "Localizing a Notch in a Steel Frame from Frequency Measurements." *J. Engrg. Mech.* 123(5) (May 1997): 422-432.

Ratcliffe, C.P. "Damage Detection Using a Modified Laplacian Operator on Mode Shape Data." *Journal of Sound and Vibration* 204(3) (1997): 505-517.

Sohn, H., and Law, K.H. "A Bayesian Probabilistic Approach for Structure Damage Detection." *Earthquake Engineering and Structural Dynamics* 26 (1997): 1259-1281.

Trimm, Marvin. "An overview of nondestructive evaluation methods." *Journal of Failure Analysis and Prevention* 3(3) (2003): 17-31.

Yoon, M.K., Heider, D., Gillespie Jr., J.W., *et al.* "Local damage detection using the two-dimensional gapped smoothing method." *Journal of Sound and Vibration* 279 (2005): 119-139.